Lyapunov-Based Model Predictive Control for Stable Operation of a 9-Level Crossover Switches Cell Inverter in Grid Connection Mode

Trabelsi, Mohamed; Makhamreh, Harnza ; Alquennah, Alamera Nouran; Vahedi, Hani

DOI
10.1109/IECON51785.2023.10312376

Publication date
2023

Document Version
Final published version

Published in
Proceedings of the IECON 2023- 49th Annual Conference of the IEEE Industrial Electronics Society

Lyapunov-based Model Predictive Control for Stable Operation of a 9-Level Crossover Switches Cell Inverter in Grid Connection Mode

Mohamed Trabelsi
Electronics and Communications Engineering Department
Kuwait College of Science and Technology
Kuwait City, Kuwait
m.trabelsi@kcst.edu.kw

Hamza Makhamreh
Department of Electrical and Electronic Engineering
Özyeğin University
Istanbul, Turkey
hamza.makhamreh@ozyegin.edu.tr

Alamera Nouran Alquennah
Department of Electrical and Computer Engineering, Texas A&M University,
College Station, TX 77843 USA
Texas A&M University at Qatar
Qatar Foundation, Doha, Qatar
alamera_nq@tamu.edu

Hani Vahedi
Department of Electrical Engineering, Mathematics, and Computer Science
Delft University of Technology
Delft, Netherlands
h.vahedi@tudelft.nl

IECON 2023- 49th Annual Conference of the IEEE Industrial Electronics Society | 979-8-3503-3182-0/23/$31.00 ©2023 IEEE | DOI: 10.1109/IECON51785.2023.10312376

***Abstract*— This study proposes the application of a Lyapunov-based Model Predictive Control (L-MPC) approach to a 9-level Crossover Switches Cell (CSC9) converter operating in grid connection mode. The proposed method utilizes the structure of the classical finite-control-set MPC (FCS-MPC) technique while integrating a cost function that requires no tuning. By deriving the cost function based on Lyapunov theory, the system stability is ensured. Notably, the suggested approach offers several advantages over traditional MPC controllers. Firstly, it eliminates the need for gain tuning, thereby simplifying the implementation process. Secondly, the proposed controller prioritizes stability as a key design aspect. The presented simulation results prove that the proposed controller effectively regulates the voltage of the DC capacitor around its desired value and feed a smooth sinusoidal current to the grid with low total harmonic distortion (THD) while operating at a unity power factor.**

Keywords—Crossover Switches Cell Converter, Multilevel Inverters, Lyapunov-based Control, Model Predictive Control, Grid-Connection.

I. INTRODUCTION

A convergence of factors and challenges has made the growing demand for renewable energy sources a global obligation. The transition to cleaner/sustainable energy sources has been sparked by the pressing need to combat climate change and reduce greenhouse gas emissions. A practical substitute for fossil fuels, renewable energy sources have the potential to reduce their negative environmental effects while still providing for society's expanding energy needs. In addition, as energy storage and grid integration technologies have advanced, the costs of renewable energy solutions have decreased, boosting their competitiveness, viability, and investment appeal [1].

In this context, grid-connected Photovoltaic (PV) systems have grown significantly in popularity in recent years as a dependable and environmentally friendly method of electricity generation. They facilitate the overall transition to a sustainable and decentralized energy system by supplying clean and renewable energy as well as helping to maintain grid stability. They are a desirable option for residential, commercial, and utility-scale applications due to their scalability, easy installation, and compatibility with current grid infrastructure, opening the way for a greener and more sustainable energy future [2].

Multilevel Inverters (MLIs) have become the preferred option in grid-connected PV applications due to their numerous advantages. MLIs use an arrangement of switching devices and capacitors/DC sources to create a staircase (multilevel) output voltage waveform, which provides various advantages compared to conventional 2-level converters such as reduced harmonic content at a lower switching frequency, ability to use standard power switches in medium/high-voltage applications, reduced switching losses, increased maximum output power, enhanced system efficiency, reduced common-mode voltage, and low dv/dt ratio [3]-[4].

Several MLI configurations have been introduced in the literature, while some of them have been widely employed in industry. The Cascaded H-bridge (CHB) topology has triggered the MLI revolution in the 1970s [5] followed by the Neutral Point Clamped (NPC) [6] and the Flying Capacitor (FC) [7] configurations. These MLI topologies have been usually considered as conventional structures and form the basis of all other complex topologies.

Considering the main development stages, the MLI topologies can be classified into two main categories. The first one consists of CHB-based inverters where the main advantage is the high modularity while the need of multiple isolated DC sources and the unequal power sharing between the cascaded power cells limits their usability [8]. The other category includes Single DC-Source (SDCS) MLI topologies such as NPC, FCI, Packed U Cell (PUC), Modular Multilevel Converter (MMC), and Crossover Switches Cell (CSC) inverters. The main advantage of these SDCS-MLIs is their ability to be fully integrated into power conversion systems where traditional 2-stage inverters are operating with no amendment requirements on the DC and AC sides and few tunings on the controller design.

However, only few SDCS-MLI topologies have been successfully employed in the industry, such as NPC [9], 3-level T-type inverter [10], ANPC [11], FCI [11], and very recently the PUC inverter [13]. Lately, a modified version of the PUC inverter, known as CSC inverter, appeared as a standalone inverter in [14], where 9 voltage levels are generated (with boosting capability) making use of 8 switching devices and 1 capacitor.

These SDC-MLIs are typically controlled by cascading voltage, current, or power loops (inner and outer loops). To achieve precise current tracking, enough control bandwidth, and quick transient operation, an inner current control is employed [15]. A voltage regulator is commonly employed in the outer loop to minimize the disturbance effect from the input and grid sides and to guarantee steady power flow. Voltage errors are further supplied to the current reference in PV systems in order to regulate the DC-link voltage. However, this might not be able to guarantee an adequate distribution of active power among the DC-links (capacitors' voltages balancing). For instance, an external regulator has been used to balance the two capacitors' voltages of NPC and T3 topologies in [16]. So, the main challenge in SDCS-MLI topologies is to track the reference of the output current while balancing the voltage of the DC capacitor. Additionally, in the majority of the SDCS-MLIs topologies such as FCI, CSC, and MMC, the state variables are interconnected and any alteration in one variable may have an impact on the other state variables. To avoid the use of external controllers, redundant switching states can be used in specific arrangements.

In this context, due to its easy implementation and high transient performance, model predictive control (MPC) has been broadly implemented to deal with multi-objective control problems of SDCS-MLIs [17]-[19] where the current system's state variables are used to predict the future ones. The principle of MPC is the optimization of a designed cost function where weighting factors are commonly used to assess the relative weight of each objective in the control decision. In order to achieve high-performance results, fine-tuning those parameters is in fact extremely important. They can be automatically computed [20]-[26] or manually tweaked by trial and error.

Alternatively, this paper proposes a Lyapunov-based MPC (L-MPC) approach to deal with the multi-objective control problem of the grid-connected CSC9 inverter under study. Indeed, Lyapunov-based control has been attracting an increased interest in power electronics systems. Such approaches offer a rigorous framework for analyzing the system behavior, designing control laws, and ensuring stability in the occurrence of disturbances and uncertainties by utilizing the principles of Lyapunov stability analysis [27]-[28]. Compared to conventional MPC strategies, the adopted approach does not require gains tuning while the cost function is designed from a stability perspective.

II. System Modelling and Control

A. System Configuration

The CSC inverter under study is presented in Fig. 1. It is worth noting that the cell switches (S_1,S_4) and (S_3,S_6) are complimentarily controlled to prevent DC capacitors short-circuits, while only one switch turns ON at the time from the middle cell switches (S_2,S_5,S_7,S_8).

As shown in TABLE I, if the voltage v_2 is controlled at $v_{dc}/3$, the 16 valid switching states (where s_i represents the ON/OFF state of the switch S_i) allow the generation of 9 distinct output voltage levels (with boosting capability) where the peak voltage corresponds to $\pm(v_{dc}+v_2)$.

B. Mathematical Modelling

In this paper, the control objectives are the supply of a smooth sinusoidal current (i_g) synchronized with the grid and the control of the voltage v_2 across the DC capacitor at its desired value. By applying the Kirchhoff's current/voltage laws, the state equations are computed by (1)-(2), and the output equation is presented by (3).

$$\frac{di_g}{dt} = \frac{1}{L}\left(v_{ab} - v_g\right) \tag{1}$$

$$\frac{dv_2}{dt} = \frac{1}{C}\left(s_3 - s_2 - s_7\right) i_g \tag{2}$$

$$v_{ab} = \left(s_1 - s_2 - s_8\right) v_{dc} + \left(s_2 - s_3 + s_7\right) v_2 \tag{3}$$

where L represents the inductance of the filter and v_g is the grid voltage.

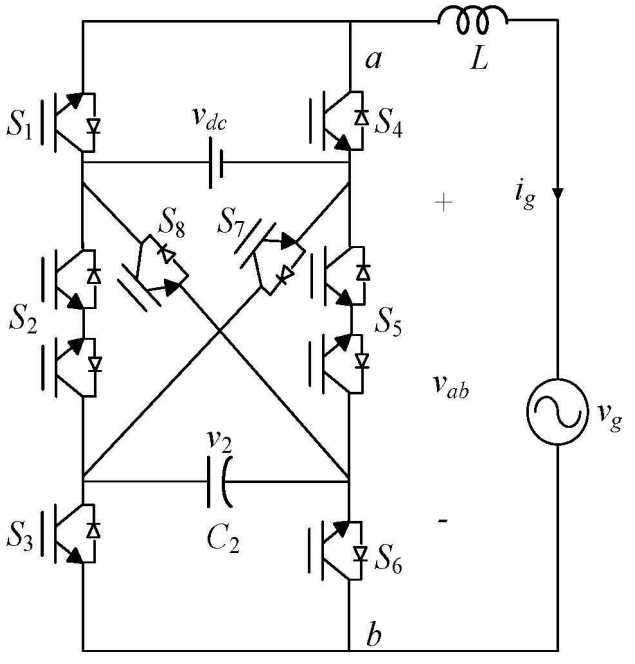

Fig. 1. System under study

TABLE I. SWITCHING PATTERNS

Switching State (n)	S_1	S_3	S_2, S_5, S_7, S_8	v_{ab}
1	1	0	0,0,1,0	$v_{dc}+v_2$
2	1	0	0,1,0,0	v_{dc}
3	1	1	0,0,1,0	
4	1	1	0,1,0,0	v_{dc} - v_2
5	0	0	0,0,1,0	v_2
6	1	0	1,0,0,0	
7	0	1	0,0,1,0	0
8	1	1	1,0,0,0	
9	0	0	0,1,0,0	
10	1	0	0,0,0,1	
11	0	1	0,1,0,0	- v_2
12	1	1	0,0,0,1	
13	0	0	1,0,0,0	- v_{dc} + v_2
14	0	0	0,0,0,1	- v_{dc}
15	0	1	1,0,0,0	
16	0	1	0,0,0,1	- v_{dc} - v_2

C. Control Design

Let's define the grid current and capacitor voltage errors as follows:

$$e_1 = i_g - i_g^{ref} \tag{4}$$

$$e_2 = v_2 - v_2^{ref} \tag{5}$$

In this paper, v_2^{ref} is set to $v_{dc}/3$ to obtain 9 output voltage levels.

A positive definite cost function (Lyapunov function) could be defined by:

$$W = \frac{1}{2}k_1 e_1^2 + \frac{1}{2}k_2 e_2^2 \tag{6}$$

It is worth noting that the gains k_1 and k_2 are selected to be real and positive numbers. As the selected Lyapunov function is positive definite, by making its derivative represented in (7) negative for all values of errors, the stability of the controlled system is guaranteed [29].

$$\dot{W} = e_1 \dot{e}_1 + e_2 \dot{e}_2 \tag{7}$$

where:

$$\dot{e}_1 = \dot{i}_g - \dot{i}_g^{ref} \tag{8}$$

$$\dot{e}_2 = \dot{v}_2 - \dot{v}_2^{ref} \tag{9}$$

By combining the previous equations with (1), (2), and (7), one can obtain:

$$\dot{W} = k_1 e_1 \left(\frac{1}{L}\left(v_{ab} - v_g\right) - \dot{i}_g^{ref} \right) + k_2 e_2 \left(\frac{1}{C}\left(s_3 - s_2 - s_7\right) i_g - \dot{v}_2^{ref} \right) \tag{10}$$

Substituting (3) in (10) and making use of the errors defined in (4) and (5) gives:

$$\dot{W} = e_1 e_2 \left(s_2 - s_3 + s_7\right)\left(\frac{k_1}{L} - \frac{k_2}{C}\right) + k_1 e_1 \left(\frac{1}{L}\left(\begin{matrix} \left(s_1 - s_2 - s_8\right) v_{dc} + \\ \left(s_2 - s_3 + s_7\right) v_2^{ref} - v_g \end{matrix} \right) - \dot{i}_g^{ref} \right) + k_2 e_2 \left(\frac{1}{C}\left(s_3 - s_2 - s_7\right) i_g^{ref} - \dot{v}_2^{ref} \right) \tag{11}$$

To eliminate the term $e_1 e_2$, k_1 is chosen to be equal to $k_2 \times L/C$. As a result, (11) can be simplified as:

$$\dot{W} = \frac{k_2}{C}\left(e_1 \left(\begin{matrix} \left(s_1 - s_2 - s_8\right) v_{dc} + \left(s_2 - s_3 + s_7\right) v_2^{ref} \\ - v_g - L\dot{i}_g^{ref} \end{matrix} \right) + e_2 \left(\left(s_3 - s_2 - s_7\right) i_g^{ref} \right) \right) \tag{12}$$

According to the Lyapunov control theorem, the controlled system will be stable for the positive definite cost function given in (6) if its derivative computed in (12) is negative.

The idea of the proposed controller is to assess the cost function given in (12) for the finite set of inputs and select the control set that corresponds to the negative value. It is worth noting that the only gain included in the cost function does not affect the minimum value selection and can be randomly set. For the sake of simplicity, k_2 is chosen to be 1, which implies having a gain-free cost function.

D. Lyapunov-based MPC

Using the first order Forward Euler approximation of (1)-(3), the discrete-time state and output equations of system are computed by:

$$i_g(k+1) = i_g(k) + \frac{T_s}{L}\left(v_{ab}(k) - v_g(k)\right) \tag{13}$$

$$v_2(k+1) = v_2(k) + \frac{T_s}{C}\left(s_3^n - s_2^n - s_7^n\right) i_g(k) \tag{14}$$

$$v_{ab}(k) = \left(s_1^n - s_2^n - s_8^n\right) v_{dc} + \left(s_2^n - s_3^n + s_7^n\right) v_2(k) \tag{15}$$

where T_s represents the sampling time, k is the sample index, and n denotes the switching pattern as indicated in TABLE I.

Moreover, the grid voltage and reference grid current are predicted at (k+1) sample using the following equations [30]:

$$v_g(k+1) = \frac{3}{2}v_g(k) - \frac{1}{2}v_g(k-1) \tag{16}$$

$$i_g^{ref}(k+1) = \frac{3}{2}i_g^{ref}(k) - \frac{1}{2}i_g^{ref}(k-1) \tag{17}$$

Then, the proposed L-MPC technique substitutes the conventional MPC cost function by the discrete-time form of the cost function given by (12) as follows:

$$\dot{W}(k+1)=\frac{k_2}{C}\left(\begin{array}{l} e_1(k+1)\left(\begin{array}{l}\left(s_1-s_2-s_8\right)v_{dc}(k)+\\ \left(s_2-s_3+s_7\right)v_2^{ref}(k)\\ -v_g-\dfrac{L}{T_s}\left(i_g^{ref}(k+1)-i_g^{ref}(k)\right)\end{array}\right)\\ +e_2(k+1)\left(\left(s_3-s_2-s_7\right)i_g^{ref}(k+1)\right)\end{array}\right) \quad (18)$$

The controller picks the switching state that corresponds to the maximum negative value of (18) and applies it to the set of switching devices. The synoptic of the proposed control approach is presented in Fig. 2.

III. Simulation Results and Analysis

In order to demonstrate the effectiveness of the proposed L-MPC technique in regulating the system variables around their references, several tests have been performed in MATLAB/Simulink using the parameters recorded in TABLE II.

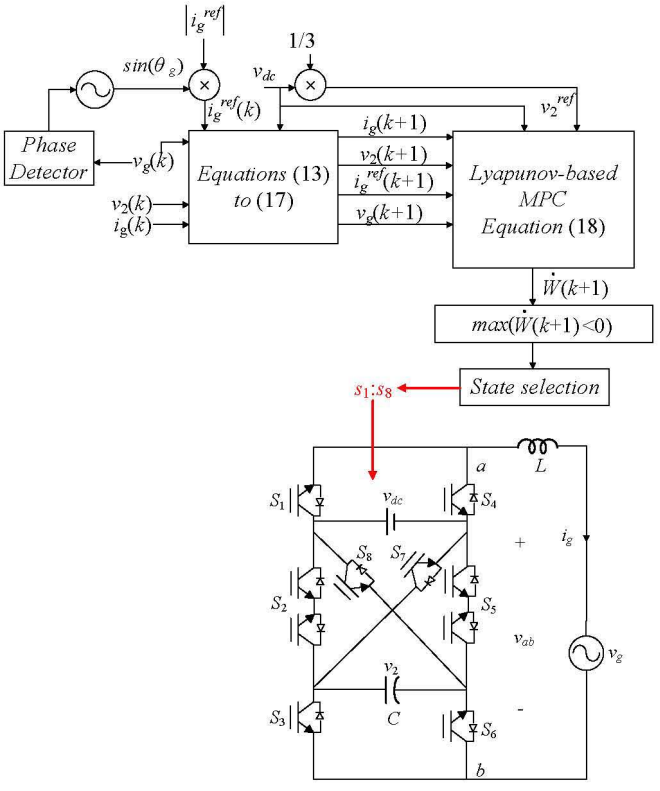

Fig. 2. Synoptic of the proposed Lyapunov-based MPC technique

TABLE II. Simulation Parameters

Designation	Value
Fundamental frequency f	50 Hz
Sampling Time T_s	20 µs
DC-Link voltage v_{dc}	300 V
Peak reference current $\lvert i_g^{ref}\rvert$	10 A
Grid Voltage v_g (rms)	240 V
Filtering Inductor L	7 mH
Fundamental frequency f	50 Hz
Capacitor C_2	2500 µF

The tracking of the voltage v_2 across the capacitor against its reference value ($v_2^{ref}=v_{dc}/3$) is shown in Fig. 3. Moreover, it can be seen that the grid current is fed with high tracking quality against its reference sinewave and unity power factor as illustrated in Fig. 4 and Fig. 5, respectively. The corresponding harmonics spectrum along with the computed THD are depicted in Fig. 6.

As expected, 9 voltage levels (Fig. 7) can be distinguished at the output terminals where the peak value of the generated output voltage (400 V) is higher than the DC-link voltage value of 300 V (boosting capability).

In Fig. 8 and Fig. 9, the transient performance of the presented L-MPC is assessed by implementing sudden step changes on the specified reference values. Fig. 8 depicts the re-tracking qualities (fast dynamic performance without overshoot) of the capacitor voltage and grid current after introducing a peak current step-up variation of 50%.

The capacitor voltage dynamic response is shown in Fig. 9 where the input voltage v_{dc} is increased from 300 V to 450 V and subsequently decreased back to 300 V (±50% of DC-link voltage variation). These findings demonstrate the strong dynamic performance of the L-MPC method in re-tracking the desired values in the presence of disturbances.

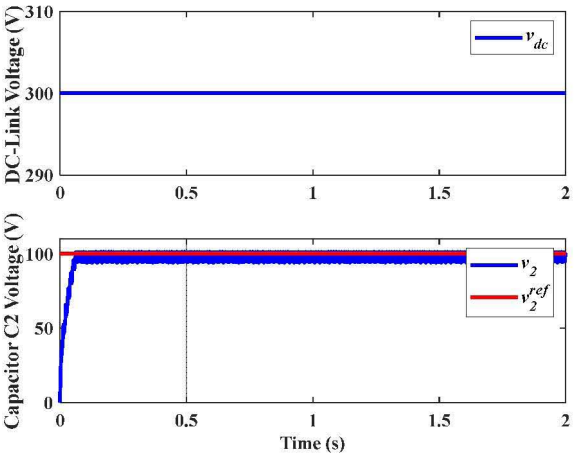

Fig. 3. Capacitor voltage tracking against its desired value

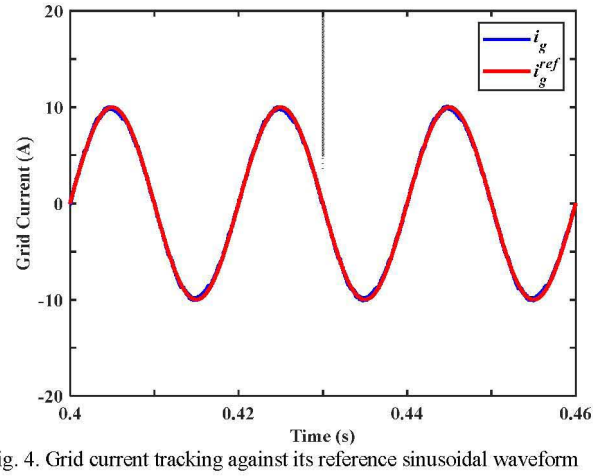

Fig. 4. Grid current tracking against its reference sinusoidal waveform

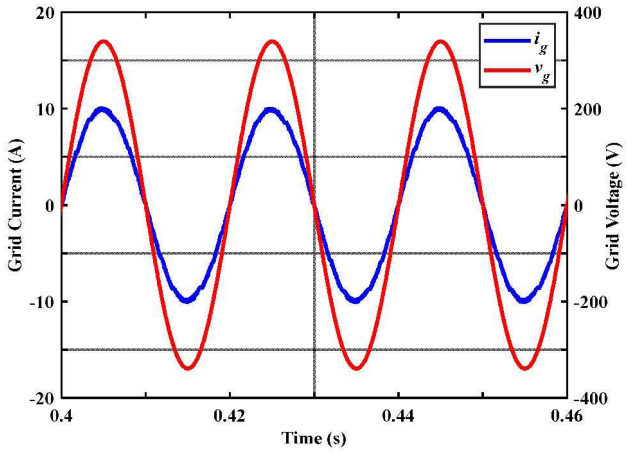

Fig. 5. Grid synchronization (unity power factor)

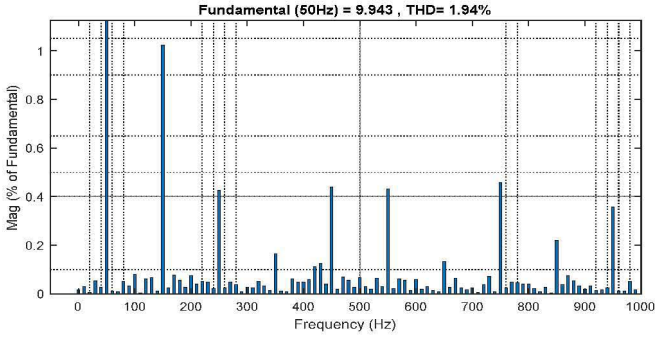

Fig. 6. Harmonics spectrum and computed current THD

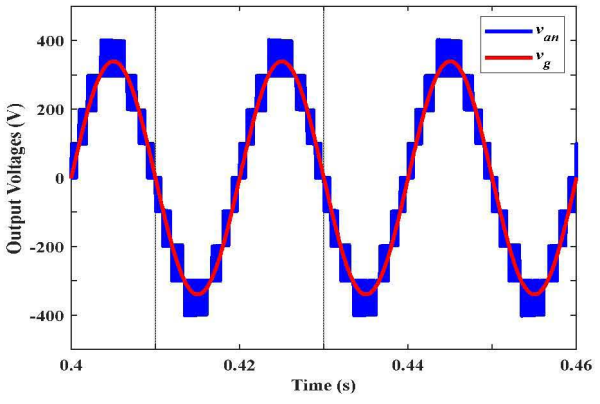

Fig. 7. The 9-level output voltage waveform versus the grid voltage

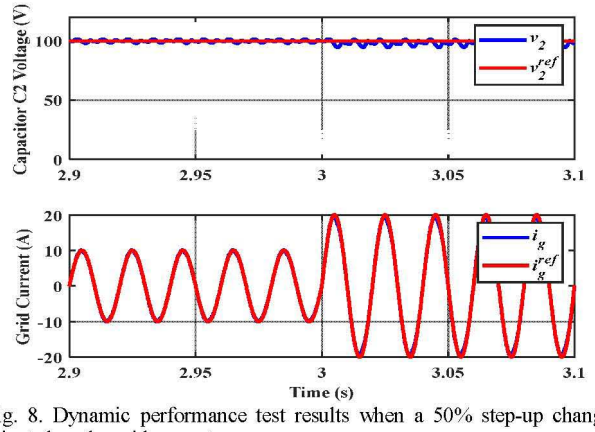

Fig. 8. Dynamic performance test results when a 50% step-up change is injected on the grid current.

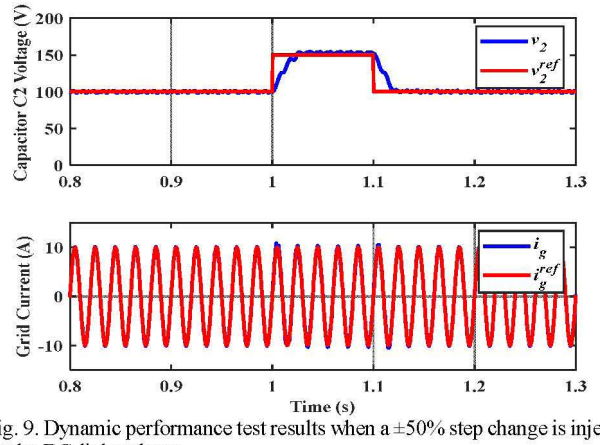

Fig. 9. Dynamic performance test results when a ±50% step change is injected on the DC-link voltage.

IV. CONCLUSIONS

This work investigated the application of a Lyapunov-based Model Predictive Control (L-MPC) technique to a Crossover Switches Cell (CSC9) converter operating in grid connection mode. The Lyapunov-based cost function was conceived from the stability perspective to minimize the errors on the grid current capacitor voltage. The proposed controller does not require any gains tuning (easy implementation under various operation conditions). The results presented in the study proves the high performance of the designed L-MPC in regulating the capacitor voltage at the reference value of $v_{dc}/3$ (to generate 9 output voltage levels) while injecting grid current with low THD synchronized with the grid voltage. Moreover, the outcomes validated the high dynamic performance of the proposed controller (claimed by Lyapunov-based control approaches) in re-tracking the desired values in the presence of disturbances (variations on the DC-link voltage and grid current reference).

REFERENCES

[1] D. Feldman, M. Zwerling and R. Margolis, "Q2/Q3 2019 Solar Industry Update," National Renewable Energy Laboratory (NREL), Colorado, USA, November 12, 2019.

[2] C. Lu, S. Guan, M. Yan, F. Zhang, K. Wu and B. Wang, "Grid Connected Photovoltaic Power Generation Station and it's Influence on Dispatching Operation Mode," *2018 2nd IEEE Conference on Energy Internet and Energy System Integration* (EI2), Beijing, 2018, pp. 1-4.

[3] J. Rodriguez, Jih-Sheng Lai and Fang Zheng Peng, "Multilevel inverters: a survey of topologies, controls, and applications," in *IEEE Transactions on Industrial Electronics*, vol. 49, no. 4, pp. 724-738, Aug. 2002, doi: 10.1109/TIE.2002.801052.

[4] Haitham Abu-Rub; Mariusz Malinowski; Kamal Al-Haddad, "Multilevel Converter/Inverter Topologies and Applications," in *Power Electronics for Renewable Energy Systems, Transportation and Industrial Applications*, IEEE, 2014, pp.422-462, doi: 10.1002/9781118755525.ch14.

[5] W. Mcmurray, "Fast response stepped-wave switching power converter circuit," May 25 1971, US Patent 3,581,212.

[6] A. Nabae, I. Takahashi, and H. Akagi, "A new neutral-point-clamped pwm inverter," *IEEE Transactions on industry applications*, no. 5, pp. 518–523, 1981.

[7] T.A. Meynard & H. Foch (1992) Multi-Level Choppers for High Voltage Applications, *EPE Journal*, 2:1, 45-50, DOI: 10.1080/09398368.1992.11463285

[8] M. Trabelsi, H. Vahedi and H. Abu-Rub, "Review on Single-DC-Source Multilevel Inverters: Topologies, Challenges, Industrial Applications, and Recommendations," in *IEEE Open Journal of the Industrial Electronics Society*, vol. 2, pp. 112-127, 2021.

[9] Three-level NPC (I-Type) (2023). Available: https://www.vincotech.com/products/by-topology/topology/three-level-npc-i-type.html.

[10] Three-level MNPC (T-Type) (2023). Available: https://www.vincotech.com/products/by-topology/topology/three-level-mnpc-t-type.html.

[11] Three-level ANPC (2023). Available: https://www.vincotech.com/products/by-topology/topology/three-level-anpc.html.

[12] Three-level FC (2023). Available: https://www.vincotech.com/products/by-topology/topology/three-level-fc-inverter.html.

[13] Five-level PUC (2023). Available : https://www.dcbel.energy/r16-specs.

[14] H. Vahedi, K. Al-Haddad, Y. Ounejjar and K. Addoweesh, "Crossover Switches Cell (CSC): A new multilevel inverter topology with maximum voltage levels and minimum DC sources," *39th Annual Conference of the IEEE Industrial Electronics Society*, Vienna, 2013, pp. 54-59.

[15] G. Elhassan, S. A. Zulkifli, E. Pathan, M. H. Khan, and R. Jackson, "A comprehensive review on time-delay compensation techniques for grid-connected inverters," *IET Renew. Power Gener.*, no. January, pp. 1–16, 2021.

[16] M. Schweizer and J. W. Kolar, "High efficiency drive system with 3-level T-type inverter," Proceedings of the 2011 14th *European Conference on Power Electronics and Applications*, Birmingham, 2011, pp. 1-10.

[17] J. Rodriguez et al., "State of the Art of Finite Control Set Model Predictive Control in Power Electronics," in *IEEE Transactions on Industrial Informatics*, vol. 9, no. 2, pp. 1003-1016, May 2013.

[18] Alquennah, A.N.; Trabelsi, M.; Rayane, K.; Vahedi, H.; Abu-Rub, H. Real-Time Implementation of an Optimized Model Predictive Control for a 9-Level CSC Inverter in Grid-Connected Mode. *Sustainability* 2021, *13*, 8119.

[19] S. Bayhan, M. Trabelsi, H. Abu-Rub and M. Malinowski, "Finite-Control-Set Model-Predictive Control for a Quasi-Z-Source Four-Leg Inverter Under Unbalanced Load Condition," in *IEEE Transactions on Industrial Electronics*, vol. 64, no. 4, pp. 2560-2569, April 2017.

[20] M. Babaie, M. Sharifzadeh, M. Mehrasa, G. Chouinard and K. Al-Haddad, "Supervised Learning Model Predictive Control Trained by ABC Algorithm for Common-Mode Voltage Suppression in NPC Inverter," in *IEEE Journal of Emerging and Selected Topics in Power Electronics*, vol. 9, no. 3, pp. 3446-3456, June 2021.

[21] L. Tang, W. Xu, X. Wang, D. Dong, X. Xiao and Y. Zhang, "Weighting Factors Optimization of Model Predictive Control Based on Fuzzy Thrust Constraints for Linear Induction Machine," in *IEEE Transactions on Applied Superconductivity*, vol. 31, no. 8, pp. 1-5, Nov. 2021.

[22] T. Dragičević and M. Novak, "Weighting Factor Design in Model Predictive Control of Power Electronic Converters: An Artificial Neural Network Approach," *IEEE Transactions on Industrial Electronics*, vol. 66, no. 11, pp. 8870-8880, 2019.

[23] M. Mohamed-Seghir, A. Krama, S. S. Refaat, M. Trabelsi and H. Abu-Rub, "Artificial Intelligence-Based Weighting Factor Autotuning for Model Predictive Control of Grid-Tied Packed U-Cell Inverter," *Energies*, vol. 13, no. 12, 2020.

[24] A. N. Alquennah, M. Trabelsi, A. Krama, H. Vahedi and M. Mohamed-Seghir, "ANN based Auto-Tuned Optimized FCS-MPC for Grid-Connected CSC Inverter," *2022 3rd International Conference on Smart Grid and Renewable Energy* (SGRE), 2022, pp. 1-6.

[25] A. N. Alquennah, M. Trabelsi and H. Vahedi, "Auto-Tuned Two-Step Horizon FCS-MPC for a Grid-Connected CSC Inverter-based PV System," *IECON 2022 – 48th Annual Conference of the IEEE Industrial Electronics Society*, Brussels, Belgium, 2022, pp. 1-6.

[26] A. Kaymanesh, A. Chandra and K. Al-Haddad, "Model Predictive Control of MPUC7-Based STATCOM Using Autotuned Weighting Factors," *in IEEE Transactions on Industrial Electronics*, vol. 69, no. 3, pp. 2447-2458, March 2022.

[27] H. Makhamreh, M. Sleiman, O. Kükrer and K. Al-Haddad, "Lyapunov-Based Model Predictive Control of a PUC7 Grid-Connected Multilevel Inverter," in *IEEE Transactions on Industrial Electronics*, vol. 66, no. 9, pp. 7012-7021, Sept. 2019, doi: 10.1109/TIE.2018.2879282.

[28] H. Makhamreh, M. Trabelsi, O. Kükrer and H. Abu-Rub, "A Lyapunov-Based Model Predictive Control Design With Reduced Sensors for a PUC7 Rectifier," in *IEEE Transactions on Industrial Electronics*, vol. 68, no. 2, pp. 1139-1147, Feb. 2021, doi: 10.1109/TIE.2020.2969122.

[29] J.-J. E. Slotine et al., Applied Nonlinear Control. Englewood Cliffs, NJ, USA: Prentice-Hall, 1991, vol. 199, no. 1.

[30] O. Kukrer, "Discrete-time current control of voltage-fed three-phase PWM inverters," in *IEEE Transactions on Power Electronics*, vol. 11, no. 2, pp. 260-269, March 1996, doi: 10.1109/63.486174.